

Solution-Processed, High-Performance Nanoribbon Transistors Based on Dithioperylene

Wei Jiang,[†] Yan Zhou,[‡] Hua Geng,[†] Shidong Jiang,[§] Shouke Yan,[§] Wenping Hu,[†] Zhaohui Wang,^{*,†} Zhigang Shuai,^{*,†} and Jian Pei^{*,†}

Beijing National Laboratory for Molecular Sciences, Key Laboratory of Organic Solids, Institute of Chemistry, Chinese Academy of Sciences (CAS), Beijing 100190, China, Key Laboratories of Bioorganic Chemistry and Molecular Engineering of the Ministry of Education, College of Chemistry, Peking University, Beijing 100871, China, and State Key Laboratory of Chemical Resource Engineering, Beijing University of Chemical Technology, Beijing 100029, China

Received August 23, 2010; E-mail: wangzhaohui@iccas.ac.cn; jianpei@pku.edu.cn; zgshuai@tsinghua.edu.cn

Abstract: Solution-processed, high-performance 1D single-crystalline nanoribbon transistors fabricated from dithioperylene are described. The integration of two sulfur atoms into the perylene skeleton induces a compressed highly ordered packing mode directed by S···S interactions. The mobilities of up to 2.13 cm² V⁻¹ s⁻¹ for a dithioperylene individual nanoribbon make it particularly attractive for electronic applications.

One-dimensional (1D) organic nano- or microstructures have been intensively developed in recent years for their high crystallinity, good processability, flexibility, and large area fabrication.¹ High performance transistors for both holes and electrons based on organic 1D structures were reported.² Remarkably, fabricating such structures with mobilities higher than 1.0 cm² V⁻¹ s⁻¹ was even achieved via solution process.³ Moreover, the chemical versatility of semiconductor molecules can be controlled by means of incorporating functionalities through rational molecular design (“molecular engineering”), which can fine-tune the molecular packing structures and thus improve the charge-carrier mobility for applications in OFETs (“crystal engineering”). However, only a few reports were focused on the device performance of the film instead of the “engineered crystals”.⁴

We present here a crystal engineering strategy to control the organization of heteroatom-annulated perylenes in the solid state that enforces cofacial π -stacking with channels for hole transport directed by chalcogen–chalcogen interactions. In our earlier work, we have demonstrated that the double-channel 1D charge transport superstructures have been successfully achieved involving perylo[1,12-*b,c,d*]thiophene (PET) and its selenophene analogue (PESE).⁵ In view of the unique structure of perylene, we would like to design and synthesize a symmetric derivative dithioperylene (**1**) with two sulfur atoms annulated on its two bay positions that will facilitate more effective charge transporting. As expected, marked S···S intercolumnar interactions of 3.45 Å were found in the solid state, and thus, a compressed highly ordered packing mode was formed. The individual nanoribbon transistors with carrier mobility as high as 2.13 cm² V⁻¹ s⁻¹ and an on/off ratio up to 10⁶ were easily fabricated utilizing this molecule by solution process.

Stimulated by the practical synthesis of PET from 1-nitroperylene,⁶ dithioperylene (**1**) was obtained via three-step reactions in about 8% overall yield. The key step in our approach involved

effective regiospecific mononitration of PET at the free bay region with an excess of HNO₃/H₂O reagent in almost 15% yield. And the desired product was synthesized as bright yellow needle-like crystals by copper-mediated dechalcogenation⁷ since the intermediate 1,2-dithiin (**2**) is preferentially produced (Scheme 1, for details see the Supporting Information).

Scheme 1. Synthesis of Dithioperylene



Considering the very limited solubility of the studied molecules in common solvents at ambient temperature, solution electrochemistry measurement of dithioperylene **1** to corroborate the HOMO values was not possible. Electronics structure has been calculated at B3LYP/6-31G(d) level by Gaussian03 software; the energy levels are -5.30 eV (HOMO) and -1.82 eV (LUMO), and hence, a very large gap of 3.48 eV is estimated. And an optical band gap of 3.12 eV is determined from an onset absorption of ~398 nm measured from UV–vis spectra (Figure S2) comparable to the above theoretical calculations. Thermogravimetric analysis (TGA) performed under nitrogen showed the onset decomposition temperature (*T*_d) at 343 °C for **1** (Figure S1). Both values indicate an exceptional thermal and chemical stability of this material.

Crystals suitable for single-crystal X-ray analysis are obtained by slow cooling of a solution of **1** in hot toluene. The crystals packed into columns along the *b*-axis direction (Figure 1). Intermolecular π - π interactions could be observed in the stacked column with the interplane distance of about 3.42 Å and the tilt angle of about 38.5°, revealing the more compressed packing and slightly more overlap of π stacks than that of PET molecules (3.47 Å and 39.8°).⁸ Most importantly, these columns were linked through S···S nonbonding interactions (3.45 Å) to form a compressed highly ordered packing mode, which makes **1** an attractive candidate for device applications.

Single-crystalline nanoribbons were fabricated by solution process in which the crystallization process was sped up to form nanosized crystals by methanol injection.^{3a} A total of 0.5 mg of powder of the compound **1** was dissolved in 1 mL of boiling tetrahydrofuran (THF) in the glove box, while 200 μ L of methanol was injected into the hot solution. The light yellow precipitations were formed within 1 h. During the process, the molecules of compound **1** self-assembled into 1D nanostructure due to the optimized π - π stacking of the aromatic plane. To elucidate the

[†] Beijing National Laboratory for Molecular Sciences.

[‡] Peking University.

[§] Beijing University of Chemical Technology.

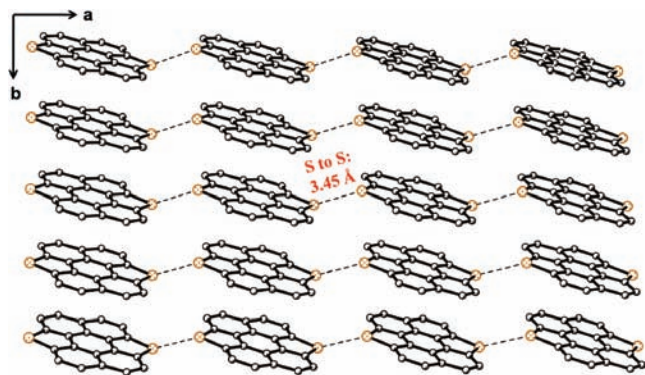


Figure 1. Packing arrangement of dithiopyrene (**1**) illustrating the ideal π - π molecular stacking along the b axis, and a compressed highly ordered packing mode induced by marked intercolumnar S \cdots S interactions within the a - b plane (hydrogen atoms were omitted for clarity).

structure of **1**, a typical transmission electron microscopy (TEM) image of a representative nanoribbon is given in Figure 2B, and

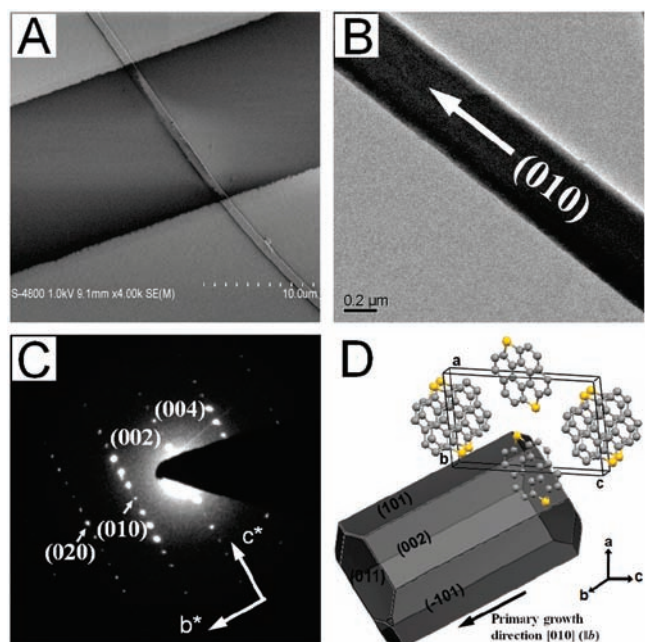


Figure 2. (A) The SEM image of the individual ribbon OFET by a plastic microfiber mask. (B) The TEM image of an individual ribbon, showing a preferential growth along the [010] direction. (C) Its corresponding SAED pattern. (D) Theoretically predicted growth morphology of a single crystal of **1**.

its corresponding selected-area electron diffraction (SAED) pattern (Figure 2C) is indexed with lattice constants obtained from the single-crystalline XRD diffraction data: $a = 9.6585(19)$ Å, $b = 4.3731(9)$ Å, $c = 15.436(3)$ Å, $\beta = 98.37(3)^\circ$. No change of the SAED pattern was observed for different parts of the same ribbon, indicating the single crystallinity of the 1D nanostructure. The diffraction spots suggest that the single-crystalline **1** nanoribbons grew along the [010] direction (i.e., b -axis). The morphology theoretically predicted by the Bravais–Friedel–Donnay–Harker (BFDH) method agreed well with the electron diffraction data, which coincided with the π - π stacking direction of dithiopyrene molecules (Figure 2D).

The suspension in THF/methanol solution was directly spin-coated onto the n -octadecyltrimethoxysilane (OTS)-treated SiO₂/Si substrate,⁹ and then, the nanoribbons were assembled onto the

substrate surface. The plastic microfiber mask was employed here to fabricate the single nanoribbon transistors.^{2c} Typical output and transfer characteristics of representative OFETs based on 1D single-crystalline nanoribbons are shown in Figure 3. All devices exhibited

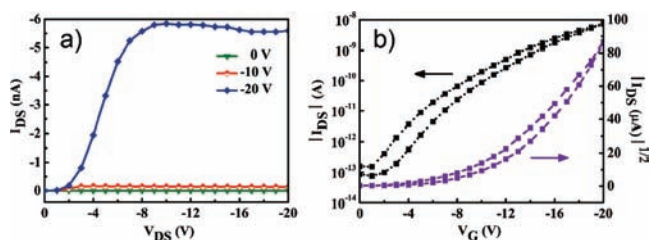


Figure 3. The electrical characteristics of the transistor based on individual microribbon of **1**: (a) output, (b) transfer characteristics of the device.

typical p-channel FET characteristics. The mobility as high as 2.13 cm² V⁻¹ s⁻¹ with on/off ratio of 10^6 was achieved, the average mobility of 18 devices was 0.45 cm² V⁻¹ s⁻¹, and the average threshold was -14 V. The value is almost 3 times higher than that of PET (0.8 cm² V⁻¹ s⁻¹),^{5a} even though the vapor-phase deposited organic single crystals generally exhibit higher quality and thus higher performance than the solution-processed crystals.¹⁰ In addition, we have carried out a first-principles calculation based on hopping model coupled with a Random Walk simulation.¹¹ We found that the room temperature hole mobility for crystal of **1** can reach 29.52 cm² V⁻¹ s⁻¹, which is a defect or disorder free limit (see Supporting Information).

In summary, we have demonstrated a molecular and crystal engineering strategy toward high-performance p-channel 1D single-crystalline nanoribbon transistors based on heteroatom-annulated perylenes. The integration of two sulfur atoms instead of one into the perylene skeleton enforces a compressed highly ordered packing mode directed by S \cdots S interactions for two-dimensional hole transport. Employing this molecule in the OFETs produced mobilities as high as 2.13 cm² V⁻¹ s⁻¹ and an on/off ratios up to 10^6 for single-crystalline nanoribbons by solution process as a consequence of more uniform symmetric molecular design. Further exploration of crystal growth and device fabrication are currently underway.

Acknowledgment. For financial support of this research, we thank the National Natural Science Foundation of China (Grant 20772131, 20721061), the 973 Program (2011CB932301), NSFC-DFG joint project TRR61, and the Chinese Academy of Sciences.

Supporting Information Available: Further experimental details, characterization data of all new compounds, information of device fabrication, as well as crystallographic data for **1** and **2** presented in CIF format. This material is available free of charge via the Internet at <http://pubs.acs.org>.

References

- (1) (a) Briseno, A. L.; Mannsfeld, S. C. B.; Jenekhe, S. A.; Bao, Z.; Xia, Y. *Mater. Today* **2008**, *11*, 38–47. (b) Zang, L.; Che, Y.; Moore, J. S. *Acc. Chem. Res.* **2008**, *41*, 1596–1608. (c) Tang, Q.; Jiang, L.; Tong, Y.; Li, H.; Liu, Y.; Wang, Z.; Hu, W.; Liu, Y.; Zhu, D. *Adv. Mater.* **2008**, *20*, 2947–2951.
- (2) (a) Briseno, A. L.; Mannsfeld, S. C. B.; Lu, X.; Xiong, Y.; Jenekhe, S. A.; Bao, Z.; Xia, Y. *Nano Lett.* **2007**, *7*, 668–675. (b) Briseno, A. L.; Mannsfeld, S. C. B.; Reese, C.; Hancock, J. M.; Xiong, Y.; Jenekhe, S. A.; Bao, Z.; Xia, Y. *Nano Lett.* **2007**, *7*, 2847–2853. (c) Zhou, Y.; Liu, W.; Ma, Y.; Wang, H.; Qi, L.; Cao, Y.; Wang, J.; Pei, J. *J. Am. Chem. Soc.* **2007**, *129*, 12386–12387. (d) Xiao, S.; Tang, J.; Beetz, T.; Guo, X.; Tremblay, N.; Siegrist, T.; Zhu, Y.; Steigerwald, M.; Nuckolls, C. *J. Am. Chem. Soc.* **2006**, *128*, 10700–10701. (e) Mas-Torrent, M.; Durkut, M.; Hadley, P.; Ribas, X.; Rovira, C. *J. Am. Chem. Soc.* **2004**, *126*, 984–985. (f) Tang, Q.; Li, H.; He, M.; Hu, W.; Liu, C.; Chen, C.; Wang, C.; Liu, Y.; Zhu, D. *Adv. Mater.* **2006**, *18*, 65–68. (g) Tang, Q.; Li, H.; Liu, Y.; Hu, W. *J. Am. Chem. Soc.* **2006**, *128*, 14634–14639. (h) Ahmed, E.; Briseno, A. L.; Xia, Y.; Jenekhe, S. A. *J. Am. Chem. Soc.* **2008**, *130*, 1118–1119.

- (3) (a) Oh, J. H.; Lee, H. W.; Mannsfeld, S.; Stoltenberg, R. M.; Jung, E.; Jin, Y. W.; Kim, J. M.; Yoo, J.-B.; Bao, Z. *Proc. Natl. Acad. Sci. U.S.A.* **2009**, *106*, 6065–6070. (b) Zhou, Y.; Lei, T.; Wang, L.; Pei, J.; Cao, Y.; Wang, J. *Adv. Mater.* **2010**, *22*, 1484–1487. (c) Kim, D. H.; Lee, D. Y.; Lee, H. S.; Lee, W. H.; Kim, Y. H.; Han, J. I.; Cho, K. *Adv. Mater.* **2007**, *19*, 678–682.
- (4) (a) Sheraw, C. D.; Jackson, T. N.; Eaton, D. L.; Anthony, J. E. *Adv. Mater.* **2003**, *15*, 2009–2011. (b) Payne, M. M.; Parkin, S. R.; Anthony, J. E.; Kuo, C.-C.; Jackson, T. N. *J. Am. Chem. Soc.* **2005**, *127*, 4986–4987. (c) Moon, H.; Zeis, R.; Borkent, E.-J.; Besnard, C.; Lovinger, A. J.; Siegrist, T.; Kloc, C.; Bao, Z. *J. Am. Chem. Soc.* **2004**, *126*, 15322–15323. (d) Gsänger, M.; Oh, J. H.; Könemann, M.; Höffken, H. W.; Krause, A.-M.; Bao, Z.; Würthner, F. *Angew. Chem., Int. Ed.* **2010**, *49*, 740–743. (e) Jiang, L.; Fu, Y.; Li, H.; Hu, W. *J. Am. Chem. Soc.* **2008**, *130*, 3937–3941. (f) Briseno, A. L.; Miao, Q.; Ling, M.-M.; Reese, C.; Meng, H.; Bao, Z.; Wudl, F. *J. Am. Chem. Soc.* **2006**, *128*, 15576–15577.
- (5) (a) Sun, Y.; Tan, L.; Jiang, S.; Qian, H.; Wang, Z.; Yan, D.; Di, C.; Wang, Y.; Wu, W.; Yu, G.; Yan, S.; Wang, C.; Hu, W.; Liu, Y.; Zhu, D. *J. Am. Chem. Soc.* **2007**, *129*, 1882–1883. (b) Tan, L.; Jiang, W.; Jiang, L.; Jiang, S.; Wang, Z.; Yan, S.; Hu, W. *Appl. Phys. Lett.* **2009**, *94*, 153306.
- (6) Jiang, W.; Qian, H.; Li, Y.; Wang, Z. *J. Org. Chem.* **2008**, *73*, 7369–7372.
- (7) (a) Schroth, W.; Hintzsche, E.; Viola, H.; Winkler, R.; Klose, H.; Boese, R.; Kempe, R.; Sieler, J. *Chem. Ber.* **1994**, *127*, 401–408. (b) Okamoto, T.; Kudoh, K.; Wakamiya, A.; Yamaguchi, S. *Org. Lett.* **2005**, *7*, 5301–5304.
- (8) Santos, I. C.; Almeida, M.; Morgado, J.; Duarte, M. T.; Alcaicer, L. *Acta Crystallogr.* **1997**, *C53*, 1640–1642.
- (9) Ito, Y.; Virkar, A. A.; Mannsfeld, S.; Oh, J. H.; Toney, M.; Locklin, J.; Bao, Z. *J. Am. Chem. Soc.* **2009**, *131*, 9396–9404.
- (10) Braga, D.; Horowitz, G. *Adv. Mater.* **2009**, *21*, 1473–1486.
- (11) (a) Coropceanu, V.; Cornil, J.; da Silva Filho, D. A.; Olivier, Y.; Silbey, R.; Brédas, J.-L. *Chem. Rev.* **2007**, *107*, 926–952. (b) Valeev, E. F.; Coropceanu, V.; da Silva Filho, D. A.; Salman, S.; Brédas, J.-L. *J. Am. Chem. Soc.* **2006**, *128*, 9882–9886. (c) Wang, L.; Nan, G.; Yang, X.; Peng, Q.; Li, Q.; Shuai, Z. *Chem. Soc. Rev.* **2010**, *39*, 423–434.

JA107599R